

A Current-Source Converter with a Hybrid Dc-dc Converter Interfacing an Electric Vehicle and a Renewable Energy Source

Catia F. Oliveira^{1,*}, Ana M. C. Rodrigues¹, Delfim Pedrosa¹, Joao L. Afonso¹ and Vitor Monteiro¹

¹ALGORITMI Research Centre, University of Minho, – Guimarães – Portugal

Abstract

The increasing demand for electricity and the impact of the consumption of fossil fuels leads to the need for approaching new alternatives of energy production, namely energy storage systems (ESS) and renewable energy sources (RES). For this purpose, this paper presents a single-phase current-source converter (CSC) with a hybrid dc-dc converter connected to the dc-link, which not only allows the interface of an electric vehicle (EV) and a RES, but also operates as shunt active power filter (SAPF). The operation as SAPF is performed through the CSC connected to the power grid, compensating some power quality problems that can occur in the electrical installation, namely current harmonics and low power factor. Moreover, the CSC can operate as a grid-tied inverter or as an active rectifier. Regarding the hybrid dc-dc converter, the main role of this power converter is to interface the CSC dc-link with the power converters for the EV and RES interfaces. As demonstrated along the paper, the CSC, combined with the hybrid dc-dc converter, allows the operation as SAPF, as well as the operation in bidirectional mode, specifically for the EV operation, and for injecting power from the RES. In this paper, the power electronics structure is described in detail, and the operating principle is introduced, supported by the description of the control algorithms. The validation results show the proper operation of the CSC as SAPF and the operation of the hybrid dc-dc converter as EV battery charger and discharger, as well as RES interface.

Keywords: Current-Source Converter, Electric Vehicle, Hybrid Dc-dc Converter, Renewable Energy Source, Power Quality.

Received on 10 October 2021, accepted on 15 February 2023 published on 16 February 2023

Copyright © 2023 Catia F. Oliveira *et al.*, licensed to EAI. This is an open access article distributed under the terms of the CC BY-NC-SA 4.0, which permits copying, redistributing, remixing, transformation, and building upon the material in any medium so long as the original work is properly cited.

doi: 10.4108/ew.v9i5.3047

1. Introduction

Last decades, the price of fuel has risen and in conjunction with the current delicate economic situation, the look for new alternatives to the traditional transport sector has been crucial. In addition, the excessive emission of greenhouse gases produced by human activities contributes to global warming and climate change, which deserve special

attention [1]. Concerning the harmful effects on the environment and the costs of fuel, electric vehicles (EV) represent an alternative solution to internal combustion engine vehicles, contributing to more sustainable mobility [2][3]. Moreover, the EV can also be managed for storing and delivering power during the intermittence of the renewable energy sources (RES). Thus, the EV can be used as an energy storage system (ESS), permitting to store the energy in periods where the RES production is excessive

*Corresponding author. Email: c.oliveira@dei.uminho.pt

and in periods of intermittence, delivering the energy back to the installation contributing to balance the power management and consumption [4]. However, the integration of the EV and RES can introduce power quality problems, such as current harmonics and low power factor, due to the required power converters to interface the power grid [5][6]. The interface of the EV and RES with the power grid is performed by an ac-dc converter and by a dc-dc converter. The dc-dc converter ensures a controllable voltage and current of the dc interfaces, whereas the ac-dc converter is responsible to guarantee sinusoidal currents with low harmonic distortion and unitary power factor [7]. On the other hand, the ac-dc converter can be voltage-source converter (VSC) or current-source converter (CSC), depending on the dc-link composition. Relatively to the CSC topology, this power converter presents as main advantages a good current control and a short-circuit protection capability. Moreover, the CSC dc-link is composed of an inductor with a longer lifetime compared with the type of capacitors used in the dc-link of the VSC, namely electrolytic capacitors. Due to these advantages, the CSC can be applied in some power electronic applications, such as in the interface of RES and EV, active power filters and motor drives [8]. Nevertheless, to maintain an acceptable level of current ripple in dc-link, it is required a large dc-link inductor for the CSC [9]. To reduce the inductance value and consequently the size and costs of this inductor, a hybrid dc-dc converter is proposed in [10] for a four-wire CSC operating as a shunt active power filter (SAPF). Considering the EV control in bidirectional mode for a smart grid perspective, the interface of a conventional CSC with EV is more difficult since the CSC is unidirectional. However, the CSC connected with a hybrid dc-dc converter on the dc-link, allows the bidirectional operation for EV applications, as it is presented in [11]. Additionally, it can also be applied as a motor driver in EV applications, as shown in [12].

Figure 1 presents a block diagram showing the CSC with a hybrid dc-dc converter for interfacing an EV and a RES. Regarding EV battery charging, several control methods can be considered aimed to preserve the battery life cycle, namely the constant current and constant voltage (CC/CV) method due to its simplicity and easy implementation [13][14]. On the other hand, for the maximum power extraction from the RES, several control algorithms can be considered. However, the maximum power point tracking (MPPT) control based on the perturb and observe strategy is the most used algorithm due to its easy implementation [15][16].

This paper is an extended version of the paper [17], where is presented a single-phase CSC combined with a hybrid dc-dc converter for interfacing an EV and a RES. Based on the power electronics structure, the interface with the power grid is only performed through the CSC. However, the combination of the CSC with the hybrid dc-dc converter presents the following operation modes,

which can be highlighted as main contributions: (i) operation as SAPF; (ii) operation as EV battery charger (the EV battery are charged by power grid); (iii) operation as EV battery discharger, where part of the stored power of the EV is injected into the power grid; (iv) operation as RES interface, injecting power into the power grid; (v) combined operation of the previous modes (for instance, charging the EV and operating as a SAPF at the same time).

In section 2 is described in detail the operating principles of both power converters. In section 3 is presented the control algorithm for the single-phase CSC, namely the compensation control theory. Moreover, it is described the control used when the hybrid dc-dc converter is operating as EV charger or discharger, or when the hybrid dc-dc converter is operating as RES interface. Section 4 presents the main simulation results of the single-phase CSC with the hybrid dc-dc converter connected to the dc-link. Finally, section 5 exposes the main conclusions.

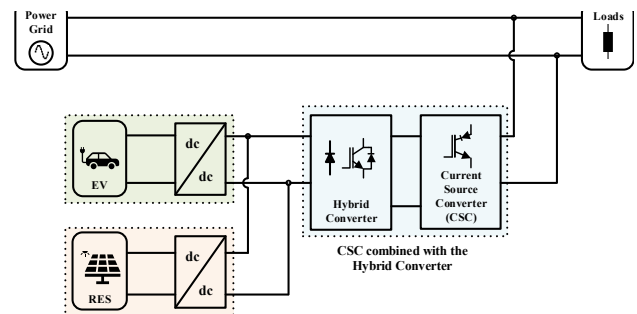


Figure 1. Block diagram of the CSC combined with the hybrid dc-dc converter connected to the dc-link, for interfacing an EV and a RES with the power grid.

2. Operating Principle of the CSC with the Hybrid Dc-dc Converter

In this section is described the topology presented in Figure 2. As can be observed, the presented structure consists of two main power stages, namely the CSC (ac-dc converter) and the hybrid dc-dc converter. The ac-dc converter is required for interfacing the power grid with the dc-link to compensate the current harmonics in the power grid and obtain a unitary power factor. This converter is composed of power semiconductors totally controlled, that it can be MOSFETs, IGBTs or RB-IGBTs. As in this power converter, the dc-link current is unidirectional, when used IGBTs, it is crucial to guarantee current reverse block, avoiding that the current flows by the antiparallel diodes of IGBTs. For that reason, the use of RB-IGBTs is a viable solution, instead of using IGBTs in series with diodes, allowing the reduction of costs and the number of electronic components [18][19]. This power converter produces three different output current values $+i_{dc}$, 0 and $-i_{dc}$, and four states of operation, such as: (1) when the current flows through the semiconductors $S1$ and $S4$

obtaining an output current of $+i_{dc}$; (2) when the current flows through the semiconductors $S2$ and $S3$ and the CSC produces an output current value of $-i_{dc}$; (3) and (4) when the current flows through the semiconductors $S1$ and $S2$ or $S3$ and $S4$ and the output current is 0. Regarding the hybrid dc-dc converter, this power converter is bidirectional and is composed of two diodes and two IGBTs. The aim of this converter is interfacing the EV, allowing the bidirectional power operation with the power grid (EV battery charging or discharging) and interfacing the RES (extracting the maximum power). Thus, the hybrid dc-dc converter has three modes of operation: (i) grid-to-vehicle (G2V) and (ii) vehicle-to-grid (V2G) and (iii) RES-to-grid. During the G2V mode, the power is transferred from the power grid to the dc-link of the hybrid dc-dc converter, where the dc-dc converter for the EV is connected. In this operation mode is applied the CC/CV method, whose output of the control is a voltage reference for the hybrid converter dc-link. On the other hand, during the V2G mode, the power is transferred from the battery to the power grid. For this operation mode, the output of the control is the voltage reference applied to the regulation of the hybrid converter dc-link. For both modes of operation, if the dc-link voltage (v_{ev}) is higher than the voltage reference, the IGBTs $S5$ and $S6$ are on, whereas if v_{ev} is lower than the voltage reference both IGBTs are off. When v_{ev} is equal to the voltage reference, it is only enabled one of the IGBTs, $S5$ or $S6$. The same is applied to the injection of power from RES to the power grid.

3. Proposed Control Algorithm

This section introduces a detailed description of the control algorithm for the single-phase CSC interfacing the EV and RES. The presented control algorithm is demonstrated in Figure 3. The control algorithm includes the control theory for the SAPF operation performed by the CSC, the EV charging using the CC/CV method and the extraction of the maximum point of the power from the RES through the MPPT control algorithm. The management of the power from/for the EV and the RES is carried out by the hybrid dc-dc converter.

The operation of the SAPF is realized before and during the EV charging and discharging and the power extraction from the RES. For the correct operation of the SAPF, it is required a method of synchronization with the power grid. In this case, it is used the E-PLL algorithm presented in [20][21], whose input signal is the power grid voltage (v_g). The dc-link regulation (p_{reg}) is obtained with a PI controller, where the input signals are the dc-link current (i_{dc}) and its reference (i_{dc}^*). Based on the E-PLL (v_{pll}) and the load current (i_L), it is calculated the compensation current (i_c) through the theory of Fryze-Buchholz-Depenbrock (FBD) presented in [22]-[24]. This control theory presents as the main advantage a simpler implementation comparing to others control theories that can be applied to SAPF, for example, the $p-q$ theory. The switching states of the power semiconductors used in CSC are obtained from the modulation block of the SAPF. The hybrid dc-dc converter is controlled for the EV charging following the two stages of the CC/CV method and for the EV discharging. As it can be observed, the variables needed to control the hybrid dc-dc converter are the EV current (i_{ev}), the EV reference current (i_{ev}^*) and the EV voltage (v_{ev}). Moreover, it is measured the voltage (v_{RES}) and the current (i_{RES}) on RES for the power calculation. Thus, it is compared the power obtained with the power calculated in the previous time to extract the maximum power and inject it into the power grid. Following, the control algorithms are described in more detail, as well as the power theories used for both converters.

3.1. Control when the CSC is Operating as SAPF

The SAPF is responsible for supplying the harmonics and reactive power required by the loads. For that, the SAPF must be capable of producing the compensation current (i_c) to obtain a power grid current sinusoidal and in phase with the power grid voltage. The i_c is calculated through a power theory, which in this case is the FBD theory. The principle of this theory is that a load can be represented by an

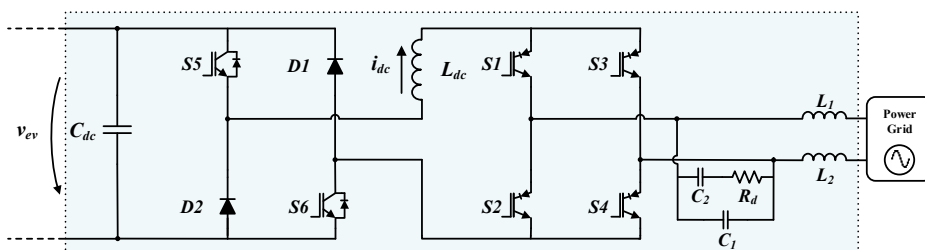


Figure 2. Electrical schematic of the single-phase CSC combined with the hybrid dc-dc converter.

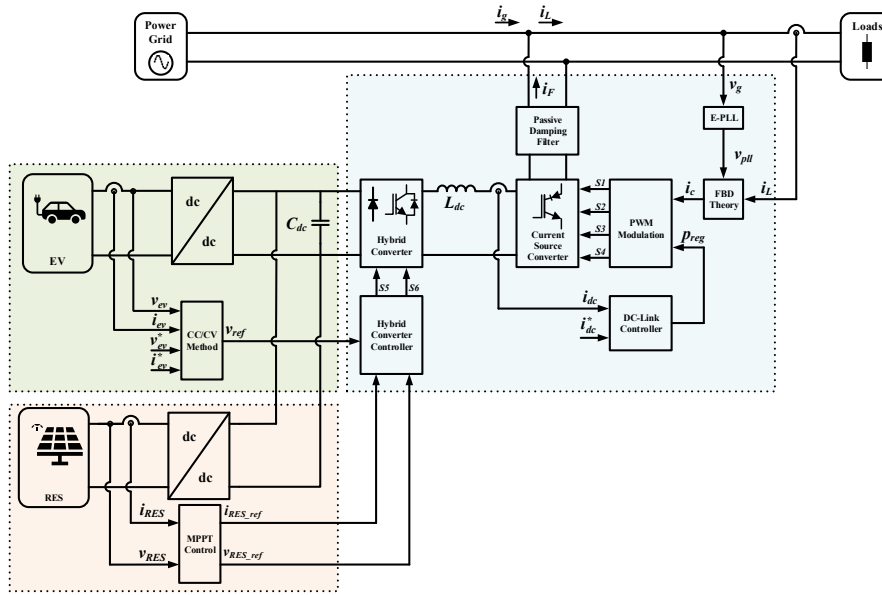


Figure 3. Block diagram of the control algorithm applied for the CSC combined with the hybrid dc-dc converter, interfacing an EV and RES with the power grid.

equivalent conductance (G_a) in parallel with a current-source. To apply this power theory, it is calculated the active power multiplying the output of the E-PLL (v_{pll}) by the load current (i_L), calculating subsequently, the average active power (P) through the sliding window method. The G_a is obtained through the P and the squared RMS value of the power grid voltage (v_g^2), as it can be seen in (1).

$$G_a = P/v_g^2 \quad (1)$$

Therefore, the active current (i_a) associated to the G_a is presented in (2).

$$i_a = G_a v_g \quad (2)$$

Finally, the compensation current produced by the SAPF is determined by (3), which corresponds to the difference between the load current (i_L) and the active current (i_a).

$$i_c = i_L - i_a \quad (3)$$

3.2. Control when the Hybrid Dc-dc Converter is Operating as EV Charger or Discharger

The hybrid dc-dc converter is bidirectional and allows the EV battery charging and discharging with a controlled current. The dc-dc converter of the EV is connected in parallel with the CSC dc-link. Due to the advantages of the CC/CV method such as its simplicity, easy implementation, and the fact that it is adequate for most

battery used in EV, this method was studied and applied in this work. Initially, it is applied a constant current for the EV and, the EV voltage increases since reaches the maximum charging voltage for the used battery. After that, the CC mode is replaced by the CV mode, where the EV current starts decreasing exponentially, maintaining the EV voltage value. The EV charging process finishes when the EV current reaches the residual battery current. During the CC mode, the error is obtained by the subtraction between the EV reference current (i_{ev}^*) and the EV current (i_{ev}). Subsequently, the error is used by the PI controller, where it is adjusted the gains, k_p and k_i , allowing that the EV current follows the established reference. The output of the PI controller is the reference voltage (v_{ev}^*) which is compared with EV voltage, whose comparison determines the states of the power semiconductors that composes the hybrid dc-dc converter. In (4) is showed the conditionals for the two IGBTs used in the hybrid dc-dc converter, S_5 and S_6 . When the maximum EV voltage is reached, the CV mode is initialized whose control is also carried out by the PI controller. In this case, the control variable is the EV voltage instead of the EV current, as previously described for the CC mode.

$$\begin{aligned} \text{If } v_{ev} < v_{ev}^*, S_5 = 0 \ S_6 = 0 \\ \text{If } v_{ev} > v_{ev}^*, S_5 = 1 \ S_6 = 1 \\ \text{If } v_{ev} = v_{ev}^*, S_5 = 0 \ S_6 = 1 \end{aligned} \quad (4)$$

3.3. Control when the Hybrid Dc-dc Converter is Operating as RES Interface

Another application of the hybrid dc-dc converter is the interface of the RES to extract the maximum power and

inject it in the power grid and/or charging the EV battery. For that, it is necessary to implement a control algorithm designated MPPT. The MPPT algorithm aims to identify constantly the maximum power point of the RES and allows that the hybrid dc-dc converter operates correctly. Several MPPT control algorithms are approached in [25][26]. The main differences presented in these MPPT algorithms are the costs, efficiency as well as the complexity of implementation. The most common MPPT algorithm is the MPPT based on the perturb and observe strategy for its simplicity and easy implementation. For the correct performance of this MPPT control algorithm, it is obtained the voltage and current values measured in the output of the RES and calculated the power values. Subsequently, the power from the RES is compared to a previous instant with a follow instant of the perturbation occurrence. Thus, it is calculated the power variation to determinate the direction of the new perturbation, i.e., if the power value, increases the next perturbation maintains the same direction, otherwise, if the power diminishes the next perturbation takes the reverse direction [27][28].

4. Simulation Results

In this section is presented the main simulation results of the topology developed in PSIM software. The presented simulations were performed for the main conditions of the CSC operation and the hybrid dc-dc converter, specifically considering the EV battery charging and discharging processes. Moreover, the simulation results include the compensation of the current harmonics and power factor in the power grid. Table 1 shows the specifications of the developed simulation model.

Initially, the hybrid dc-dc converter had as the main contribution the reduction of the inductance value of the inductor in dc-link of the CSC. However, the following results prove that the same converter apart from allowing the reduction of the inductor in dc-link, the hybrid dc-dc converter is also advantageous to interface other dc systems, like the interface of an EV and a RES. To validate the CSC operating as SAPF and the EV charging process, the presented simulation results in this paper consist of: (i) Dc-link current regulation; (ii) Compensation of current harmonics and low power factor in the power grid, by the CSC operating as SAPF; (iii) EV charging and discharging along with the harmonic compensation by the CSC operating as SAPF.

As a nonlinear load connected to the power grid, it was considered a full-bridge rectifier with a RC load (168 Ω , 2.6 mF), with a coupling inductor of 0.5 mH, as well as a RL load in parallel (12.5 Ω , 70 mH). Table 2 shows the specifications of the dc-link of both converters, including the values of components that compose the passing damping filter. This coupling filter was introduced to reduce the losses and the electromagnetic interference caused by the CSC as approached in [29].

Table 1. Specifications of the CSC interfacing EV and RES.

PARAMETERS	Value	Unit
RMS Grid Voltage	230 \pm 10%	V
Grid Frequency	50 \pm 1%	Hz
Output dc Voltage	450	V
Switching Frequency	40	kHz

Table 2. Specifications of the power converters.

PARAMETERS	Value	Unit
Inductor L_{dc}	100	μ H
Capacitor C_{dc}	300	μ F
Damping Resistor R_d	15	Ω
Inductors L_1, L_2	20	μ H
Capacitor C_1	5	μ F
Capacitor C_2	20	μ F

One of the roles of the CSC is to control and maintain the dc-link current according to the established reference value. The dc-link current (i_{dc}) is presented in Figure 4, which is regulated through the PI controller. As it can be observed, when starts the EV charging, i.e., during the transient-state operation, the dc-link current decreases, however, the dc-link current quickly reaches the reference current of 50 A.

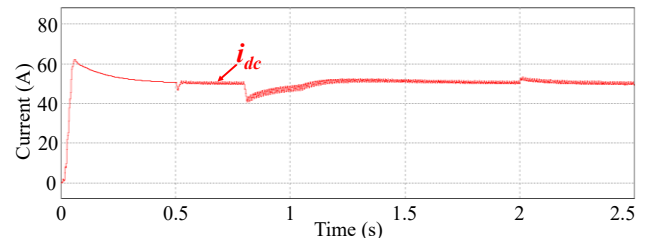


Figure 4. Simulation results of the dc-link current regulation (i_{dc}) of the single-phase CSC.

Figure 5 presents the simulation results of the power grid voltage (v_g) and grid current (i_g) before compensation. As it can be observed, the i_g is not sinusoidal and is not in phase with the v_g . The i_g presents a THD_{%f} of 36%. The RMS value of the i_g is 10.28 A. As mentioned above, the presence of harmonic distortion in the power grid can result in increasing losses, and consequently, damage the equipment connected to the installation.

After the dc-link regulation, the SAPF produces a compensation current to compensate the current harmonics and low power factor in the power grid. Figure 6 shows v_g and i_g after compensation, where the power grid current is almost sinusoidal and in phase with the power grid voltage. The RMS value of the i_g is 7.35 A. The THD_{%f} in the power

grid current is reduced from 36% to 5.69%, corresponding to an important improvement.

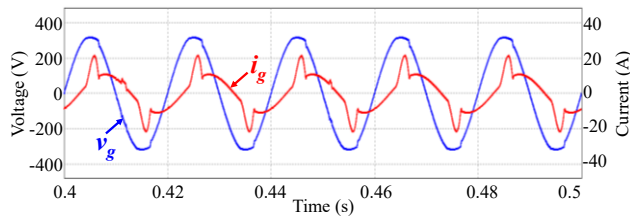


Figure 5. Simulation results of the power grid voltage (v_g) and grid current (i_g) before compensation, and without the EV charging process and injection of power from RES. The RMS value of i_g is 10.28 A.

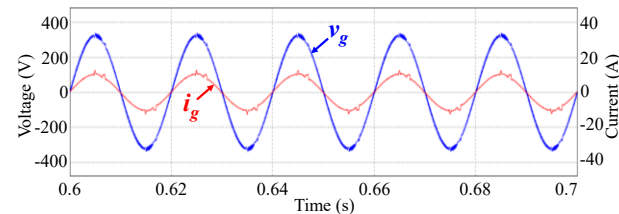


Figure 6. Simulation results of the power grid voltage (v_g) and grid current (i_g) after compensation, and without the EV charging process and injection of power from RES. The RMS value of i_g is 7.35 A.

Figure 7 shows the G2V (1 and 2) and V2G (3) modes, where i_{ev} is the EV current and v_{ev} is the EV voltage. During G2V operation mode, the EV is charged for a reference current of 10 A with a minimum voltage of 250 V. The EV charging process consists of two charging stages, namely constant current (1) followed by constant voltage (2). Initially, the EV is charged with a current of 10 A, whose power is supplied by the power grid and the RES. When the voltage in the EV reaches the maximum voltage of 450 V, the EV current starts decreasing until reaches approximately 0 A. This method is very advantageous for lithium battery charging, which is very common in EV. During V2G mode, the power from the EV is injected into the power grid for a reference current of 2 A, which corresponds to stage (3). As it can be observed during the discharging of the EV, the v_{ev} decreases. During all modes (1, 2 and 3), the CSC is controlled to operate as SAPF, i.e., compensates the current harmonics in the power grid and obtain an approximately unitary power factor.

During the EV charging and injection of power in the power grid, it cannot be neglected the power quality improvement. So, the SAPF continues operating and the current harmonics in power grid are compensated. In Figure 8 is showed v_g and i_g after compensation during EV charging process. The power grid current presents a low THD_{of} of 2.48%, which is very reduced, as it is intended.

On the other hand, the RMS value of the i_g increases to 26.7 A.

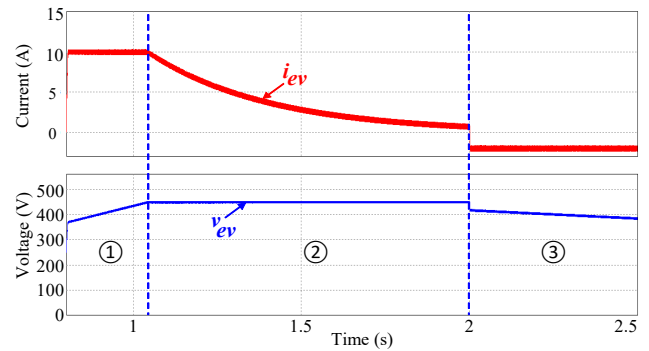


Figure 7. Simulation results of a Lithium battery charging and discharging processes: (1) CC stage; (2) CV stage and (3) EV discharging.

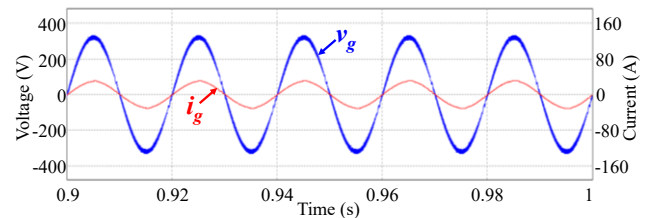


Figure 8. Simulation results of the power grid voltage (v_g) and grid current (i_g) after compensation, and during the EV charging process without injection of power from RES. The RMS value of i_g is 26.7 A.

Finally, it is carried out the injection of power from RES, where it is also effectuated the compensation of the current harmonics in the power grid side. Figure 9 presents the v_g and i_g after compensation, where i_g is in phase with v_g , whose THD_{of} value is 7.91%. As intended, the RMS value of the i_g is reduced from 7.35 A to 4 A.

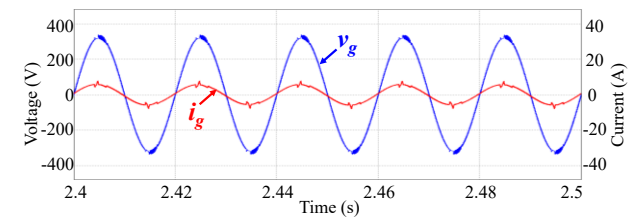


Figure 9. Simulation results of the power grid voltage (v_g) and grid current (i_g) after compensation, and during the injection of power in the power grid from RES. The RMS value of i_g is 4 A.

5. Conclusions

This paper presents a single-phase current-source converter (CSC) with a hybrid dc-dc converter on the

dc-link to interface an electric vehicle (EV) and a renewable energy source (RES). The CSC can be controlled as a shunt active power filter (SAPF) for compensating current harmonics and low power factor. The compensation of some power quality problems is realized using the FBD power theory. Furthermore, the CSC together with the hybrid dc-dc converter allows the interface of EV and RES. Regarding the EV battery charging, it was adopted the constant current and constant voltage (CC/CV) control. This method was chosen since it is adequate to lithium battery, preserving the battery lifetime. In relation to the RES interface, it was implemented a maximum power point tracking algorithm based on the perturbation and observation strategy. The topology and the operating principles are described along the paper, and a detailed description of the simulation results is presented. Initially, it is carried out the dc-link current regulation of the CSC, followed by the compensation of current harmonics in the power grid. Subsequently, it is performed the EV battery charging for a reference current of 10 A, and the EV battery discharging for a reference current of 2 A. Finally, it is injected power from the RES into the power grid using the MPPT control. For both situations, the power quality problems, namely current harmonics and low power factor are compensated. In conclusion, the obtained results show the correct operation of the CSC operating as SAPF, as well as for the interface of the EV and RES.

Acknowledgements.

This work has been supported by FCT – Fundação para a Ciência e Tecnologia within the Project Scope: UIDB/00319/2020. This work has been supported by the FCT Project newERA4GRIDS PTDC/EEI-EEE/30283/2017 and the FCT Project DAIPSEV PTDC/EEI-EEE/30382/2017.

References

- [1] J. Li, X. Zhang, S. Ali, and Z. Khan, "Eco-innovation and energy productivity: New determinants of renewable energy consumption," *Journal of Environmental Management*, vol. 271, p. 111028, 2020.
- [2] L. González, E. Siavichay, and J. Espinoza, "Impact of EV fast charging stations on the power distribution network of a Latin American intermediate city," *Renewable and Sustainable Energy Reviews*, vol. 107, pp. 309–318, 2019.
- [3] J. L. Afonso, L. A. Cardoso, D. Pedrosa, T. J. Sousa, L. Machado, M. Tanta, and V. Monteiro, "A Review on Power Electronics Technologies for Electric Mobility," *Energies*, vol. 13, no. 23, p. 6343, 2020.
- [4] Vítor Monteiro, João C. Ferreira, Andrés A. Nogueira Melendez, José A. Afonso, Carlos Couto, João L. Afonso, "Experimental Validation of a Bidirectional Three-Level dc-dc Converter for On-Board or Off-Board EV Battery Chargers", *IEEE IECON 2019 - Annual Conference of the IEEE Industrial Electronics Society*, Lisbon, Portugal, pp.3468-3473, 2019.
- [5] T. Strasser, F. André, J. Kathan, C. Cecati, C. Buccella, P. Siano, V. Mařík, "A review of architectures and concepts for intelligence in future electric energy systems". *IEEE Transactions on Industrial Electronics*, 62(4), 2424-2438, 2014.
- [6] P. S. Moses, S. Deilami, A. S. Masoum, and M. A. S. Masoum, "Power quality of smart grids with plug-in electric vehicles considering battery charging profile," *IEEE PES Innov. Smart Grid Technol. Conf. Eur. ISGT Eur.*, pp. 1–7, 2010.
- [7] Vítor Monteiro, Tiago J. C. Sousa, M. J. Sepúlveda, Carlos Couto, António Lima, João L. Afonso, "A Proposed Bidirectional Three-Level dc-dc Power Converter for Applications in Smart Grids: An Experimental Validation", *IEEE SEST 2019 - International Conference on Smart Energy Systems and Technologies*, Porto, Portugal, pp.1-6, 2019.
- [8] X. Guo, Y. Yang, and X. Zhang, "Advanced control of grid-connected current source converter under unbalanced grid voltage conditions," *IEEE Transactions on Industrial Electronics*, vol. 65, no. 12, pp. 9225–9233, 2018.
- [9] X. Guo, Y. Yang, and X. Wang, "Optimal space vector modulation of current-source converter for DC-link current ripple reduction," *IEEE Transactions on Industrial Electronics*, vol. 66, no. 3, pp. 1671–1680, 2018.
- [10] S. Pettersson, M. Salo, and H. Tuusa, "Optimal DC current control for four-wire current source active power filter," *Conf. Proc. - IEEE Appl. Power Electron. Conf. Expo. - APEC*, pp. 1163–1168, 2008.
- [11] G. J. Su and L. Tang, "Current source inverter based traction drive for EV battery charging applications," *2011 IEEE Veh. Power Propuls. Conf. VPPC 2011*, pp. 1–6, 2011.
- [12] L. Tang and G. J. Su, "Boost mode test of a current-source-inverter-fed permanent magnet synchronous motor drive for automotive applications," *2010 IEEE 12th Work. Control Model. Power Electron. COMPEL 2010*, 2010.
- [13] W. Shen, T. T. Vo, and A. Kapoor, "Charging algorithms of lithium-ion batteries: An overview," *Proc. 2012 7th IEEE Conf. Ind. Electron. Appl. ICIEA 2012*, pp. 1567–1572, 2012.
- [14] J. S. Moon, J. H. Lee, I. Y. Ha, T. K. Lee, and C. Y. Won, "An efficient battery charging algorithm based on state-of-charge estimation for electric vehicle," *2011 Int. Conf. Electr. Mach. Syst. ICEMS 2011*, 2011.
- [15] A. K. Abdelsalam, A. M. Massoud, S. Ahmed, and P. N. Enjeti, "High-performance adaptive perturb and observe MPPT technique for photovoltaic based microgrids," *IEEE Trans. Power Electron.*, vol. 26, no. 4, pp. 1010–1021, 2011.
- [16] T. ESRAM and P. L. Chapman, "Comparison of Photovoltaic Array Maximum Power Point Tracking Techniques," *IEEE Trans. Energy Convers.*, vol. 22, no. 2, pp. 439–449, 2007.
- [17] Catia F. Oliveira, Ana M. C. Rodrigues, Delfim Pedrosa, Joao L. Afonso and Vitor Monteiro, "A Single-Phase Current-Source Converter Combined with a Hybrid Converter for Interfacing an Electric Vehicle and a Renewable Energy Source," *EAI SESC 2020*, 2020.
- [18] M. Routimo, M. Salo, and H. Tuusa, "Comparison of voltage-source and current-source shunt active power filters," *IEEE Trans. Power Electron.*, vol. 22, no. 2, pp. 636–643, 2007.
- [19] M. Salo and S. Pettersson, "Current-source active power filter with an optimal DC current control," *PESC Rec. - IEEE Annu. Power Electron. Spec. Conf.*, 2006.
- [20] M. Karimi-Ghartemani, S. A. Khajehoddin, P. K. Jain, A. Bakhshai, and M. Mojiri, "Addressing DC component in pll and notch filter algorithms," *IEEE Trans. Power Electron.*, vol. 27, no. 1, pp. 78–86, 2012.

- [21] M. Karimi-Ghartemani and M. R. Iravani, "A method for synchronization of power electronic converters in polluted and variable-frequency environments," *IEEE Trans. Power Syst.*, vol. 19, no. 3, pp. 1263–1270, 2004.
- [22] L. S. Czarnecki, "Budeanu and Fryze: Two frameworks for interpreting power properties of circuits with nonsinusoidal voltages and currents," *Electr. Eng.*, vol. 80, no. Teoria de Potência, pp. 359–367, 1997.
- [23] J. Zhou, Z. Wang, and X. Fu, "Study on the improved harmonic detection algorithm based on FBD theory," *Asia-Pacific Power Energy Eng. Conf. APPEEC*, no. 1, pp. 2–5, 2011.
- [24] V. Staudt, "Fryze - Buchholz - Depenbrock: A time-domain power theory," in *International School on Nonsinusoidal Currents and Compensation (ISNCC)*, pp. 1–12, 2008.
- [25] D. Sera, R. Teodorescu, J. Hantschel, and M. Knoll, "Optimized maximum power point tracker for fast-changing environmental conditions," *IEEE Trans. Ind. Electron.*, vol. 55, no. 7, pp. 2629–2637, 2008.
- [26] S. Li, B. Zhang, T. Xu, and J. Yang, "A new MPPT control method of photovoltaic grid-connected inverter system," in *The 26th Chinese Control and Decision Conference (2014 CCDC)*, pp. 2753–2757, 2014.
- [27] Motahhir, Saad, Aboubakr El Hammoumi, and Abdelaziz El Ghzizal. "The most used MPPT algorithms: Review and the suitable low-cost embedded board for each algorithm," *Journal of cleaner production*, 2020.
- [28] S. Baraskar, S. K. Jain, and P. K. Padhy, "Fuzzy logic assisted P and O based improved MPPT for photovoltaic systems," *Int. Conf. Emerg. Trends Electr. Electron. Sustain. Energy Syst. ICETEESES 2016*, pp. 250-255, 2016.
- [29] N. Hensgens, M. Silva, J. A. Oliver, J. A. Cobos, S. Skibin, and A. Ecklebe, "Optimal design of AC EMI filters with damping networks and effect on the system power factor," *2012 IEEE Energy Convers. Congr. Expo. ECCE 2012*, vol. 7, no. 2, pp. 637–644, 2012.